Mitochondrial Recombination and Introgression during Speciation by Hybridization

Jean-Baptiste Leducq,*[,†,1,2] Mathieu Henault,[†,1] Guillaume Charron,[1] Lou Nielly-Thibault,[1] Yves Terrat,[2] Heather L. Fiumera,[3] B. Jesse Shapiro,[2] and Christian R. Landry*[,1]

[1]Institut de Biologie Intégrative et des Systèmes, Département de Biologie, PROTEO, Pavillon Charles-Eugène-Marchand, Université Laval, Québec, QC, Canada

[2]Département des Sciences Biologiques, Pavillon Marie-Victorin, Université de Montréal, Montréal, QC, Canada

[3]Department of Biological Sciences, Binghamton University, Binghamton, NY

[†]These authors contributed equally to this work.

***Corresponding authors:** E-mails: jeanbaptiste.leducq@gmail.com; christian.landry@bio.ulaval.ca.

Associate editor: Patricia Wittkopp

Abstract

Genome recombination is a major source of genotypic diversity and contributes to adaptation and speciation following interspecies hybridization. The contribution of recombination in these processes has been thought to be largely limited to the nuclear genome because organelles are mostly uniparentally inherited in animals and plants, which prevents recombination. Unicellular eukaryotes such as budding yeasts do, however, transmit mitochondria biparentally, suggesting that during hybridization, both parents could provide alleles that contribute to mitochondrial functions such as respiration and metabolism in hybrid populations or hybrid species. We examined the dynamics of mitochondrial genome transmission and evolution during speciation by hybridization in the natural budding yeast *Saccharomyces paradoxus*. Using population-scale mitochondrial genome sequencing in two endemic North American incipient species *SpB* and *SpC* and their hybrid species *SpC, we found that both parental species contributed to the hybrid mitochondrial genome through recombination. We support our findings by showing that mitochondrial recombination between parental types is frequent in experimental crosses that recreate the early step of this speciation event. In these artificial hybrids, we observed that mitochondrial genome recombination enhances phenotypic variation among diploid hybrids, suggesting that it could play a role in the phenotypic differentiation of hybrid species. Like the nuclear genome, the mitochondrial genome can, therefore, also play a role in hybrid speciation.**

Key words: **mitochondrial recombination, speciation by hybridization, *Saccharomyces*.**

Introduction

Hybridization between closely related species generates new gene combinations that may lead to reproductive isolation of hybrid individuals with the parental species and the emergence of novel phenotypes (reviewed in Schumer et al. 2014). These new combinations are made possible by the recombination of the parental genomes. Unlike the nuclear genome, the genomes of organelles in Eukaryotes (mitochondria and chloroplasts) are predominantly inherited in a uniparental manner (reviewed in Barr et al. 2005), mostly from the maternal parent in the case of mitochondrial genomes (mtDNAs). Assuming that the progeny resulting from hybridization between two species (or diverged populations) inherits only one of the parental mtDNAs, one expects that the co-occurrence of both parental mtDNA types in the progeny (heteroplasmy) is rare and that recombination in the mitochondrial genome is thus very limited in most Eukaryotes. Exceptions to maternal mtDNA inheritance however exist, for instance in the case of biparental inheritance of mtDNAs (Breton and Stewart 2015), allowing for recombination to take place. The observation of spontaneous heteroplasmy or recombinant mtDNAs in experimental hybrids (Kondo et al. 1990; Gyllensten et al. 1991) and natural populations (Kvist et al. 2003; Jaramillo-Correa and Bousquet 2005; Xu et al. 2009) also indicates that paternal mtDNA may be transmitted along with maternal mtDNA occasionally even in species that normally exhibit maternal inheritance. These observations suggest that biparental (or rare biparental) inheritance during interspecific hybridization could be followed by recombination between mtDNAs (Rokas et al. 2003), which has the potential to generate new combinations of genes and haplotypes with functional consequences for mitochondrial function.

Fungi show a large diversity of mtDNA inheritance patterns (Wilson and Xu 2012; Xu and Wang 2015). For instance, in the budding yeast *Saccharomyces cerevisiae*, mtDNA transmission is biparental such that the two mating cells contribute to the zygote mtDNAs. This heteroplasmic state is transient, as vegetative segregation leads to the fixation of a single haplotype in the hybrid cell lineage within a few dozen cell divisions (Birky et al. 1978; Birky 2001). However, recombination between parental mtDNAs can occur at a high rate

Article

during this short heteroplasmic transition (Fritsch et al. 2014). Unlike many other model eukaryotes, mtDNA from *Saccharomyces* species is highly variable both within and between species, and both intergenic and coding regions contribute to phenotypic variation (Paliwal et al. 2014; Wolters et al. 2015). This indicates that mitochondrial recombination could contribute to novel genotypes and phenotypes in the hybrid progeny.

Closely related species from the genus *Saccharomyces* can be crossed with each other in the laboratory, and many interspecific hybridization events occurred during the domestication of *Saccharomyces* by humans for brewing and winemaking (Landry et al. 2006; Hittinger 2013). The mtDNA analysis of these experimental and industrial strains revealed many contrasting features of the mitochondrial transmission dynamics after hybridization. On the one hand, some cases of strong biased transmission have been reported. For instance, the absence of the *S. cerevisiae* mitochondrial type in *S. cerevisiae* × *S. uvarum* hybrid brewing strains suggests the preferential transmission and/or the postmating selection of the *S. uvarum* parental haplotype (Piskur et al. 1998; Kodama et al. 2006; Rainieri et al. 2008). However, under laboratory conditions, the *S. cerevisiae* mtDNA is preferentially transmitted in *S. cerevisiae* × *S. uvarum* hybrids, potentially caused by a higher number of replication origins (*ori* sequences) in the *S. cerevisiae* mtDNA (Lee et al. 2008) or asymmetrical incompatibilities. On the other hand, some studies have shown that there might not be inherent biases in transmission. The study of hybrid wine strains has shown that mtDNA from either parent can be transmitted (reviewed in Querol and Bond 2009).

The aforementioned cases suggest that, despite the high mitochondrial recombination rate observed within species, for instance in *S. cerevisiae* (Fritsch et al. 2014), mitochondrial recombination in interspecific crosses is null or limited. A possible explanation is that one parental mitochondrial type is rapidly eliminated after hybridization, before mitochondrial recombination effectively occurs. However, since many of these studies focused on a single locus for genotyping, the extent of mitochondrial recombination could not be assessed. Recently, Peris et al. (2017) observed that the transfer of specific mitochondrial genes may have occurred among *Saccharomyces* species, revealing a potential history of recombination in the mitochondrial genome. Most of these reported cases occurred in domesticated and sometimes distantly related species. It is thus still unclear to what extent mitochondrial recombination occurs in natural populations and whether it can contribute to phenotypic variation during the process of speciation by hybridization. To examine this question, we need to examine ongoing or recent events in natural populations.

We recently showed that a new yeast species arose through hybridization in wild populations of *Saccharomyces paradoxus* (Leducq et al. 2016), a budding yeast that thrives on the bark of deciduous trees and the associated soil in Eurasia and America (Sniegowski et al. 2002) (fig. 1*A*). In the northeast of its distribution in North America, we identified two lineages, *SpB* and *SpC*, that show growth phenotypes consistent with local climatic adaptations (Leducq et al. 2014) and nucleotide divergence (2%) that support a scenario where a population split was initiated prior to or during the last glaciation event 100 Kya (Leducq et al. 2016; fig. 1*B*). These two lineages show strongly reduced fertility in F1 hybrids, show a large array of distinct growth phenotypes and a limited geographical overlap, suggesting that they are incipient species (Leducq et al. 2014, 2016). Population genomic analyses recently showed that these two incipient species hybridized in their contact zone after the glacial retreat and gave rise to a third incipient species, *SpC**, which is genetically and phenotypically distinct from *SpB* and *SpC*, and also partially reproductively isolated (Leducq et al. 2016). A significant fraction of the reproductive isolation of the parental lineages with each other (Charron et al. 2014) and with the hybrid lineages could be attributed to abnormal chromosomal segregation (Leducq et al. 2016) but other mechanisms such as Bateson–Dobzhansky–Muller incompatibilities (BDMIs) could also contribute. Here, we examine mitochondrial genome evolution during this recent event of speciation by hybridization. We show that the hybrid lineage displays largely the same bias in terms of parental contributions to the mitochondrial and nuclear genomes, and that it carries a recombinant mitochondrial haplotype with a specific genome content and configuration. We demonstrate that when hybridization is reproduced in the laboratory, recombination between mtDNA parental haplotypes contributes to increase phenotypic variation of hybrid strains.

Results and Discussion

We previously found that the nuclear genome of the hybrid lineage *SpC** was ~95% inherited from its parental lineage *SpC*, indicating that *SpC** has experienced more backcrosses with *SpC* than with *SpB* after the original hybridization event or that it has preferentially lost *SpB* haplotypes by selfing or mitotic loss of heterozygosity (Leducq et al. 2016; fig. 1*B*). This observation suggests that, even if the original hybrid was heteroplasmic for *SpC* and *SpB* mtDNAs, repeated backcrosses with *SpC* could have eliminated the *SpB* mitochondrial type from the *SpC** lineage. In order to test this hypothesis, we examined mitochondrial haplotypes in the *SpC** and parental lineages by analyzing polymorphism in the mitochondrial genomes of 127 *S. paradoxus* strains from the American lineages *SpB* ($n = 81$), *SpC* ($n = 34$), and *SpC** ($n = 12$). The lineage assignment of 127 strains was done based on 14,974 nuclear SNPs and whole-genome phylogeny (Leducq et al. 2016) (Supplementary information 1). A phylogeny based on 254 high-quality mitochondrial SNPs revealed that the three lineages form distinct groups (see supplementary fig. S1*A*, Supplementary Material online), with all strains from lineage *SpC* and most of the *SpC** strains (92%) forming a monophyletic group, as observed for the nuclear genome (Leducq et al. 2016). This observation is congruent with a scenario under which backcrosses between *SpC** and its parental lineages most likely occurred with *SpC*, resulting in the rapid elimination of the *SpB* mitochondrial haplotype during the evolution of the *SpC** lineage. One

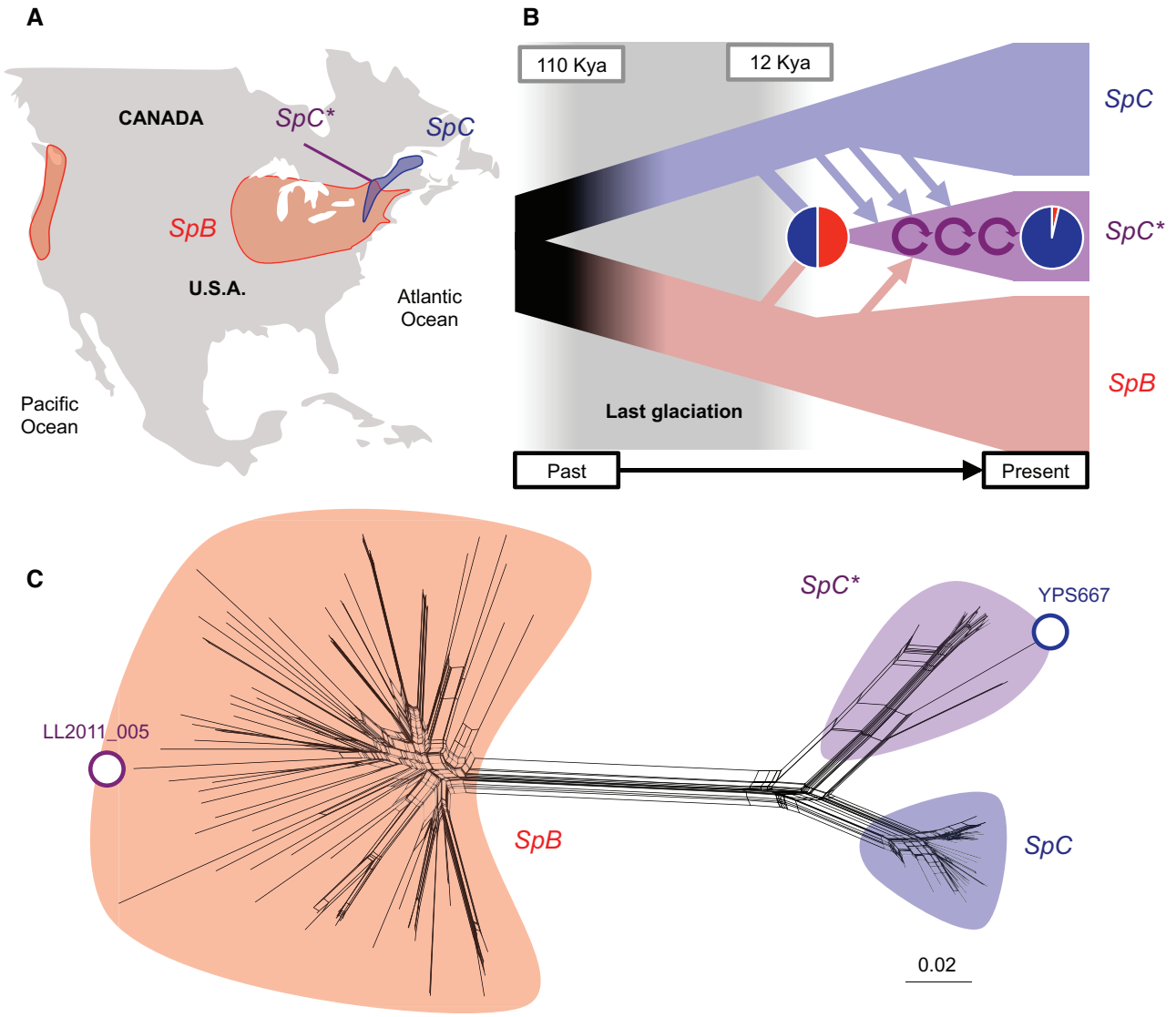

Fig. 1. mtDNA inheritance after speciation by hybridization between two North-American *S. paradoxus* lineages is mostly uniparental. (*A*) The hybrid incipient species *SpC** (purple) is mostly found in the overlap of the distribution area of its two parental lineages *SpB* (red) and *SpC* (blue) in North-America. (*B*) *SpC** arose from the initial hybridization between *SpB* and *SpC* during secondary contact after the last glaciation (~12,000 years ago). The pie chart represents the evolution of the relative proportions of *SpB*- and *SpC*-like nuclear polymorphisms in *SpC**. The initial hybridization event was followed by more frequent backcrosses with the *SpC* than with the *SpB* parent (straight arrows) or by repeated selfing and selection within the hybrid lineage (curved arrows) as suggested by the low proportion of *SpB*-like nuclear polymorphism in *SpC** (~3.7%). (*C*) A Splitstree of 134 mtDNA sequences based on 254 polymorphic sites reveals the reticulate evolution of *SpC** and YPS667 (*SpC*) mtDNA, suggesting recombination between *SpB* and *SpC* mtDNA types in the hybrid lineage, with the exception of LL2011_005 that inherited the *SpB* mtDNA type.

*SpC** strain (LL2011_005) clusters with the *SpB* lineage, indicating that although rare, backcrosses between *SpC** and *SpB* may have occurred and led to the elimination of the *SpC* mitochondria in some *SpC** strains, or that the *SpB* mitochondrial haplotype is still segregating in the *SpC** lineage since the initial hybridization event. Splitstree (fig. 1*C*) and STRUCTURE analyses (see supplementary fig. S1*B*, Supplementary Material online) based on the same limited number of polymorphic sites reveal admixture within and among *SpB* and *SpC** clades, indicating a more complex evolutionary history than suggested by the phylogeny (see supplementary fig. S1*A*, Supplementary Material online). Interestingly, the *SpC* strain YPS667 clusters with *SpC** in a phylogeny based on these sites. The nuclear genome of this strain was shown to be divergent from other *SpC* strains (0.14% of nucleotide divergence) and to have admixed regions with the *SpC** hybrid lineage (Leducq et al. 2016). This observation indicates that the YPS667 mitochondria could have been inherited from *SpC** through gene flow between *SpC* and *SpC** after the formation of the hybrid lineage (Leducq et al. 2016). These crosses could have been possible due to the incomplete reproductive isolation between *SpC* and *SpC** (Leducq et al. 2016).

The limited number of SNPs used for the analyses performed above are due to the fact that many genomes have been sequenced at low coverage, which leads to a small number of sites of high quality across the entire sample, making it

difficult to dissect the potential recombination events between the parental mtDNA that led to the *SpC** mitochondrial genomes. We therefore used high-coverage data to analyze 20 complete mtDNA from the *S. paradoxus SpB* ($n = 11$), *SpC* ($n = 6$), and *SpC** ($n = 3$) lineages to examine the pattern of mitochondrial inheritance in the hybrid lineage *SpC** (Supplementary information 1). We included, as outgroups, 18 complete mtDNA sequences from *S. paradoxus* Asian ($n = 2$) and European lineages (*SpA*; $n = 6$), *S. cerevisiae* ($n = 4$) and the *Saccharomyces eubayanus* complex species ($n = 6$) to identify potential horizontal transfers or ancient hybridization events that could explain the patterns of introgression described above (see Supplementary information 1; table S1, Supplementary Material online). The assignment of strains to species and to *S. paradoxus* lineages was previously done based on whole-genome phylogenies and complete mtDNA sequences were retrieved from previous studies (Foury et al. 1998; Wei et al. 2007; Nakao et al. 2009; Prochazka et al. 2012; Baker et al. 2015; Wolters et al. 2015; Wu and Hao 2015; Leducq et al. 2016; Okuno et al. 2016) (see Supplementary information 1; table S1, Supplementary Material online). We improved the assembly of 22 mtDNA previously assembled with ABySS (Leducq et al. 2016; mean number of scaffolds, $n_S = 4.5 \pm 6.1$), using the software IDBA_ud (Peng et al. 2012; $n_S = 1.1 \pm 0.3$; see supplementary table S2, Supplementary Material online; accession numbers KY287641–KY287662). We obtained the RFLP band patterns after EcoRV digestion expected from our assembly for each lineage of North American strains, confirming the overall accuracy of the mtDNA assemblies (see supplementary fig. S2, Supplementary Material online).

An analysis of pairwise synteny revealed that mitochondrial genomes are colinear within *S. paradoxus* American lineages and with *S. cerevisiae*, but not with *S. paradoxus* Eurasian lineages mtDNAs (*SpA* and Asia; fig. 2*A*). This result is surprising considering that mtDNA is syntenic within *S. cerevisiae* (Wolters et al. 2015) and within the *S. eubayanus* complex species (Okuno et al. 2016). We thus report here the first case of mtDNA rearrangement within a *Saccharomyces* species. The synteny between the *S. cerevisiae* and *S. paradoxus* American lineages suggests that the *S. cerevisiae*-like mtDNA architecture is ancestral in *S. paradoxus* and that rearrangements occurred in the Eurasian lineages (fig. 2*B*). Another possibility is that the mtDNA architecture is derived in the American lineages and was inherited from *S. cerevisiae* by hybridization after the split between American and Eurasian populations, which would be supported by the fact that the *S. paradoxus* American lineages inherited some mtDNA elements such as *cox3* from *S. cerevisiae* by horizontal gene transfer (HGT) or during an ancient hybridization event (Peris et al. 2017). However, this former study only included the *SpB* lineage, so we cannot conclude whether the mtDNA transferred from *S. cerevisiae* to *S. paradoxus* occurred before or after the divergence between *SpB* and *SpC*.

To test if ancient hybridization or HGT have affected the population structure and the architecture of the complete American *S. paradoxus* mtDNA or only affected some loci, we annotated the 38 complete mtDNAs and performed a phylogeny based on an alignment of concatenated sequences of coding elements (CDS; see supplementary fig. S3, Supplementary Material online). The global phylogeny confirms that the American *S. paradoxus* lineages form a monophyletic group (see supplementary fig. S3*A*, Supplementary Material online), which is also supported by a STRUCTURE analysis (see supplementary fig. S3*B* and *C*, Supplementary Material online). Surprisingly, the Eurasian *S. paradoxus* lineages cluster with *S. cerevisiae*, confirming that the two species experienced mtDNA recombination during ancient hybridization or HTG (Peris et al. 2017). To look in greater details at the regions that were affected by these recombination events and whether these recombination events took place before or after the divergence between Eurasian and American *S. paradoxus* lineages, we performed separated phylogenies of aligned nucleotide sequences for each CDS and mobile elements (introns and maturase-like genes) identified in the 38 mtDNA, using *S. cerevisiae* and *S. eubayanus* as outgroups (fig. 3). For each locus, *S. paradoxus* American strains share more similarity with each other than with any outgroup, suggesting that the *S. paradoxus* American lineages did not receive any major recent contribution from external lineage or species since their divergence with Eurasian lineages. A phylogeny of the mitochondrial gene *cox3* (fig. 3*A*) confirms that the *S. paradoxus* American lineages show a higher nucleotide similarity to *S. cerevisiae* (98.76%) than to the Eurasian lineages (97.41%), indicating that the hybridization event that lead to the transfer of *cox3* from the *S. cerevisiae* mtDNA to that of *S. paradoxus* (Peris et al. 2017) may have affected the American *S. paradoxus* mtDNA architecture, but the higher *SpB-SpC* similarity (99.21%) suggests that it took place before the *SpB-SpC* divergence. A similar phylogenetic signal for *atp6* suggests that this gene also experienced transfers between *S. cerevisiae* and *S. paradoxus* American lineages (fig. 3*A*). Our analysis revealed that *S. paradoxus* Eurasian lineages and *S. cerevisiae* share more similarity for *cob* (fig. 3*B*; 98.19%) and *cox1* (fig. 3*C*; 97.61%) than with *S. paradoxus* American lineages (97.56 and 97.35%, respectively), suggesting that the same or an independent ancestral recombination event between *S. cerevisiae* and *S. paradoxus* also affected the mtDNA architecture of Eurasian lineages. Overall, these results show that the architecture of the mitochondrial genome, which is known to vary between species (Aguileta et al. 2014), can also rapidly evolve within species, and that mitochondrial recombination following hybridization with other species is a major contributor to this evolution.

The aforementioned mtDNA recombination events occurred before the hybridization between *SpB* and *SpC*, and thus unlikely affected the relatively recent evolution of the *SpC** mtDNA. Interestingly, the phylogeny of concatenated mitochondrial CDS reveals that the hybrid lineage *SpC** and strain YPS667 cluster with *SpB* (see supplementary fig. S3, Supplementary Material online), which is in contradiction with the phylogeny based on high-quality mitochondrial SNPs (see supplementary fig. S1*A*, Supplementary Material online). These conflicting phylogenies suggest that *SpC** and YPS667 mtDNAs result from recombination events between

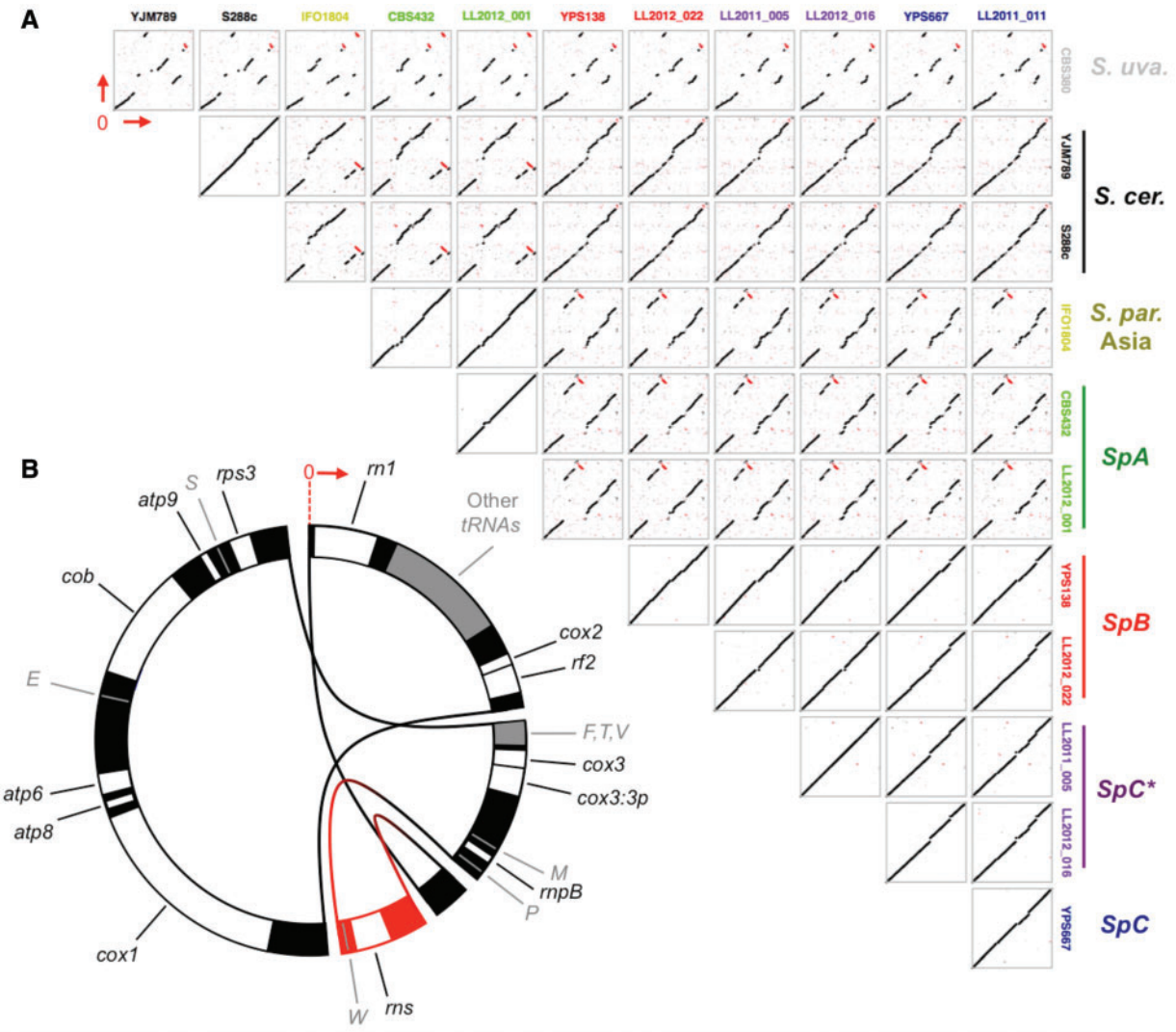

Fig. 2. Major mtDNA rearrangements occurred within *Saccharomyces paradoxus* after divergence between Eurasian and American lineages. (*A*) The comparison of 12 complete *Saccharomyces* mitochondrial genomes reveals the complete synteny between American *S. paradoxus* lineages and *S. cerevisiae* but rearrangements between the *S. paradoxus* American and Eurasian lineages (grey: *S. uvarum*; black: *S. cerevisiae*; yellow: *S. paradoxus* Asian lineage; green: *SpA*; red: *SpB*; purple: *SpC**; blue: *SpC*). Each dot indicates 100% identity between two unique 20 bp sequences. Red dots indicate inversions. The alignment origin (0 and red arrows) corresponds to the first nucleotide of *rn1*. (*B*) Schematized architecture of the *S. cerevisiae* and American *S. paradoxus* mtDNA types. White boxes indicate CDSs, grey boxes indicate tRNAs labeled with the corresponding amino-acid (letters). Breaks and curves indicate rearrangements that occurred after the divergence between American and Eurasian *S. paradoxus* lineages (inversion in red).

parental lineages *SpB* and *SpC*, which is also supported by the reticulate evolution of the *SpC** and YPS667 mtDNA types in the Splitstree analysis (fig. 1C). To identify the relative contributions of *SpB* and *SpC* mtDNA types and the regions that were affected by recombination, we identified phylogenetic discrepancies in gene-by-gene phylogenies among *S. paradoxus* strains (fig. 3). This analysis revealed that most of the *cox1* exons and introns were systematically inherited from *SpC* in all *SpC** and YPS667 (fig. 3C), whereas *cob* introns and exons and *atp6* were systematically inherited from *SpB* (fig. 3A and *B*). The analysis of other regions confirmed that the *SpC** strain LL2011_005 inherited most of its mitochondrial genes from *SpB*, whereas other *SpC** strains and YPS667 inherited these genes from *SpC* (fig. 3D). Within *S. paradoxus* American mtDNA types, we observed extensive presence–absence polymorphism of mobile elements, including introns in the *cox1* and *cob* genes (see supplementary fig. S4A, Supplementary Material online), which resulted in extensive variation in terms of size and GC content in American *S. paradoxus* mtDNA relative to outgroups (see supplementary fig. S4*B* and *C*; Supplementary information 2, Supplementary Material online). Most intronic elements in *cob* and the maturase-like gene *rf3* (located 3′ of *atp6*) are shared between *SpB* and *SpC** but absent from *SpC*, whereas some introns from genes *cox1* and a maturase-like gene located in 3′ of *cox3* (*cox3:3p*) are present in both *SpB* and *SpC* but absent from *SpC**. As observed above, the *SpC* strain YPS667 has the same profile as *SpC** for *cox3:3p*, *rf3* and *cox1* introns

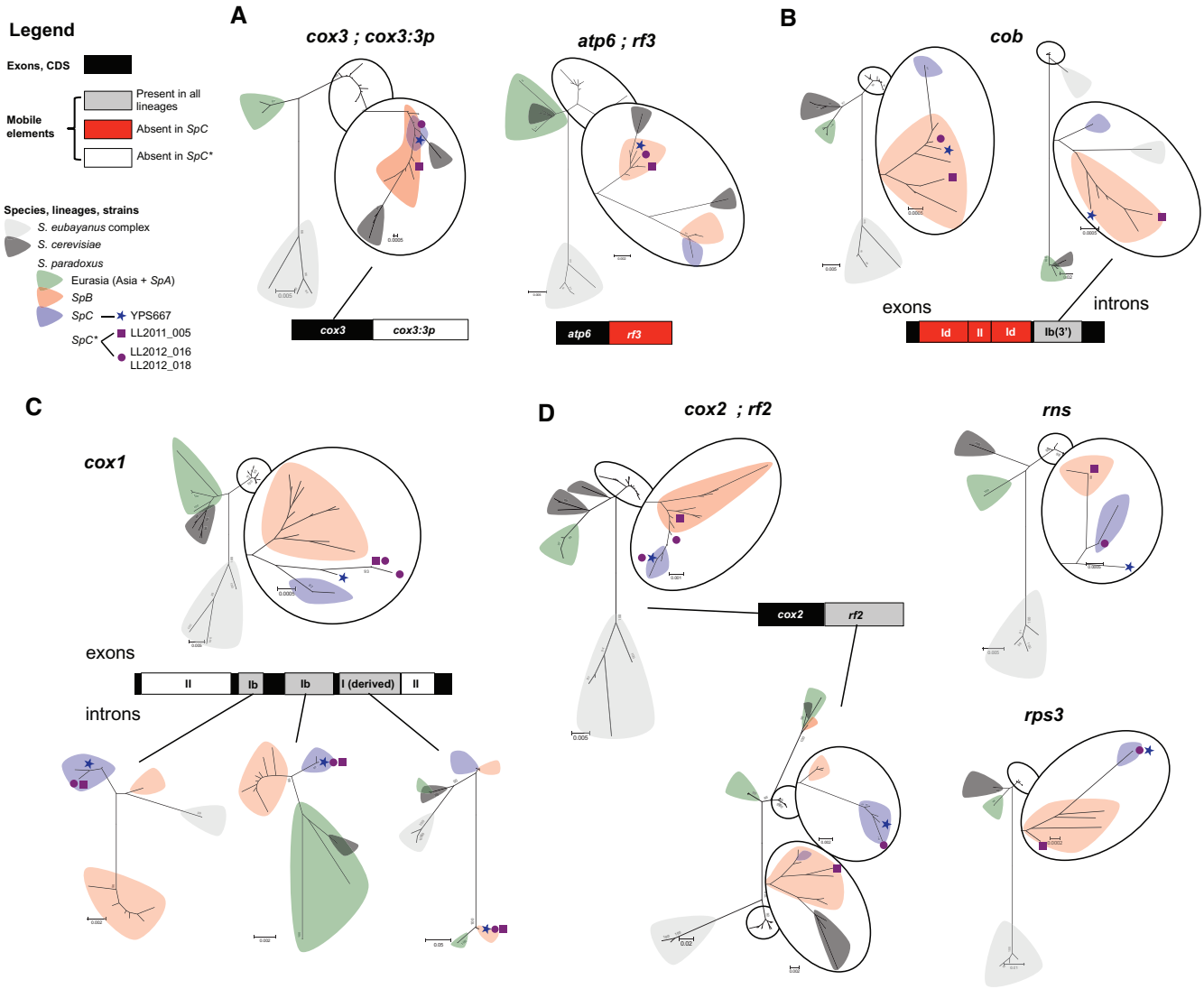

FIG. 3. *SpC** mtDNA results from introgression with uneven contributions from parental mitochondrial types *SpB* and *SpC*. Pattern of introgression for fixed (CDS, exons) and mobile (introns, maturase-like genes) mitochondrial elements, revealed by phylogenies (nucleotide sequences; maximum composite likelihood model, 1,000 permutations) among 38 strains. Branches are highlighted according to species and *S. paradoxus* lineages (legend on top left). *SpC** strains and YPS667 are labeled with specific symbols. Phylogenies were not displayed for mobile elements when absent from *SpC** (white boxes) or only present in *SpC** and *SpB* (red boxes). Branches with American *S. paradoxus* lineages are magnified in circles. (*A*) Detailed phylogenies of *cox3* and *atp6* suggest mitochondrial recombination after ancient hybridization between *S. cerevisiae* and *S. paradoxus* American lineages. The positions of *SpC** strains and YPS667 suggest that they inherited *atp6* and *cox3* from *SpB*, independently from this ancient hybridization event. (*B*) *SpC** and YPS667 inherited *cob* from lineage *SpB*. Most of *cob* introns and the *rf3* maturase are only present in *SpB* and *SpC**. (*C*) *SpC** and YPS667 mostly inherited *cox1* from lineage *SpC*. (*D*) The inheritance of other mitochondrial genes varies among *SpC** strains.

(see supplementary fig. S4*A*, Supplementary Information 2, Supplementary Material online). Overall, the presence–absence polymorphism in introns in *SpC** follows the pattern of polymorphism in mitochondrial CDS, suggesting that recombination that followed hybridization between *SpB* and *SpC* is tightly linked with the dynamics of mobile elements. Mitochondrial mobile elements were previously showed to promote recombination during horizontal gene transfer between fungal and plant mtDNA (Beaudet et al. 2013) and our observations suggest that these elements could also be involved in the generation of recombined mtDNA types after hybridization.

Taken together, mobile elements and CDS only represent 22.8–30.9% of the total mtDNA length so we extended the analysis to the entire mtDNA. We therefore performed the alignment of 20 complete mtDNAs from the three American lineages to examine in details how polymorphism inherited from *SpB* and *SpC* segregated in *SpC** and YPS667 mtDNAs. A STRUCTURE analysis performed on 2052 polymorphic sites from this alignment revealed that *SpB* and *SpC* mtDNAs (including YPS667) belong to two distinct populations (see supplementary fig. S5*A* and *B*, Supplementary Material online). As observed from phylogenies for most of mitochondrial genes (fig. 3), *SpC** strains LL2012_016 and LL2012_018 were assigned to the *SpC* population whereas LL2011_005 was mostly assigned to *SpB*, with little contribution from *SpC* (7%), confirming that *SpC** mitochondria received

uneven contributions from the two parental types. We calculated relative frequencies of ancestral haplotypes inherited from *SpB* and *SpC* along discrete 750bp windows of the *SpC** and YPS667 mtDNAs (see supplementary fig. S5C, Supplementary Material online). This analysis indicates that 87% of the LL2011_005 mtDNA was inherited from *SpB*, whereas this proportion represents only 13–17% of the LL2012_016, LL2012_018, and YPS667 mitochondria. This polymorphism is not evenly distributed along the mitochondrial genome (see supplementary fig. S5C, Supplementary Material online). Different mitochondrial haplotypes were thus produced by recombination early in the initial hybridization events and are still segregating today in *SpC** or were produced after the hybridization event through backcrosses with the parental lineages.

Recombination in *SpC** mtDNAs after hybridization required the simultaneous presence of *SpB* and *SpC* mtDNAs in a single cell, which is compatible with biparental mtDNA inheritance followed by recombination. To experimentally validate this in *S. paradoxus*, we created diploid hybrids between *SpB* and *SpC* and analyzed the mtDNA haplotype inherited by each of these independently derived hybrid strains. We generated 18 independent *SpB* × *SpC* diploid hybrids (see supplementary table S3, Supplementary Material online) and analyzed their mtDNA restriction fragments length polymorphisms (mtRFLPs) to determine in each case if mtDNA was inherited from the *SpB* or *SpC* parent or corresponded to a recombinant haplotype. To strengthen the identification of mtDNA haplotypes, mtRFLPs analysis were performed with two restriction enzymes whose sites are distributed all along the genome (see supplementary fig. S6*A*, Supplementary Material online). Eight hybrid strains (44%) exhibited mtRFLPs that were distinct from the parental profiles (because of shifted, missing or new bands; supplementary fig. S6*B* and *C*, Supplementary Material online), indicating that these hybrids have recombinant mtDNA haplotypes.

Among the hybrids with recombinant mtDNA haplotypes, three exhibited identical mtRFLPs profiles for the two enzymes (ud_01, ud_04, and ud_09), whereas the five remaining hybrids exhibited visible differences for either or both enzymes (see supplementary fig. S6*B* and *C*, Supplementary Material online). An analysis based on the restriction maps of *SpB* and *SpC* mtDNAs revealed that the three hybrids with identical mtRFLPs have mostly *SpC*-like haplotypes with an *SpB* introgression spanning from ~55–65 kb on the mtDNA alignment (see supplementary figs. S6*B* and *C* and S7, Supplementary Material online). Five hybrids (28%) had mtRFLPs identical to *SpB* and five (28%) were identical to *SpC*, suggesting the inheritance of parental, that is, non-recombinant, haplotypes. To support this result, we performed two independent PCR assays targeting polymorphic mtDNA loci between *SpB* and *SpC* and confirmed that the 10 hybrids with non-recombinant mtRFLP profiles have PCR profiles consistent with the parental haplotypes (see supplementary fig. S6*D* and *E*, Supplementary Material online). It is possible that many recombination events were undetected because of the inability of mtRFLPs analysis to reveal changes that preserve sequence length between restriction sites. Therefore, we cannot rule out the possibility that haplotypes classified as parental contain introgressions. Nevertheless, the obvious signatures of recombination observed in almost half of the hybrids show that mtDNA recombination is frequent in experimental crosses, although inheritance of parental mtDNAs is also likely possible.

The previously described diploid *SpB* × *SpC* hybrids harbor a completely heterozygous nuclear genome and are thus isogenic, excepted for the mitochondrial genome. Although rare nuclear mitotic recombination events cannot be ruled out because of the number of cell divisions required to produce homoplasmic hybrids, the phenotypic variation associated with such events should affect all the strains with equal probability, regardless of their mitochondrial haplotype. Therefore, any phenotypic variation observed in these hybrids between parental and recombinant haplotypes can be confidently attributed to genetic variation in the mitochondrial genome. Using colony size on high-density colony arrays as a proxy for growth rate, we measured phenotypic variation among the 18 experimental hybrids strains in 15 environmental conditions that cover combinations of three incubation temperatures (30, 35 and 37 °C) and five carbon or nitrogen sources (glucose, ethanol, glycerol, maltose, and allantoin). Within each combination of mitochondrial haplotype category (*SpB*, *SpC*, or recombinant) and environmental condition, we performed a one-way ANOVA to test for a significant contribution of interstrain variation to the overall growth rate variation (Supplementary materials 3 and 4). We found that for most environmental conditions, the fraction of overall growth variation attributable to interstrain variation within the *SpB*, *SpC* or recombinant category is larger for the strains harboring recombinant mitochondrial haplotypes than either parental haplotypes (higher ANOVA *F*-statistic value; fig. 4*A*, Supplementary information 4, Supplementary Material online). The condition for which this effect is strongest (maximum *F* value) is at 37 °C with glycerol, a non-fermentable carbon source that requires mitochondrial respiration for growth (fig. 4*A*, *C*). These results suggest that the frequent mitochondrial recombination occurring in *S. paradoxus* hybrids may contribute to phenotypic variation in these strains.

There is compelling evidence that genetic interactions between mtDNA and the nuclear genome can affect various metabolic, regulatory or life-history traits and play a role in hybrid breakdown between species or populations (Burton et al. 2013; Barreto et al. 2015; Paliwal et al. 2014; Zhu et al. 2014; Latorre-Pellicer et al. 2016; Mossman et al. 2016). The variation observed here could thus be caused by direct genotype-to-phenotype effects or through genetic interactions with the nuclear genome or among loci within the mtDNA. We note that much of the phenotypic variation associated with recombinant mtDNAs appears to yield reduced growth rates (fig. 4*B*). These altered growth phenotypes could result from negative epistatic interactions among mitochondrial alleles of the two parental populations within the recombinant haplotypes. Another possibility is that in the hybrid strains each mitochondrial locus (either from *SpB* or *SpC*) can interact with a full set of related nuclear alleles in the heterozygous nuclear genome, leading to potential dominant

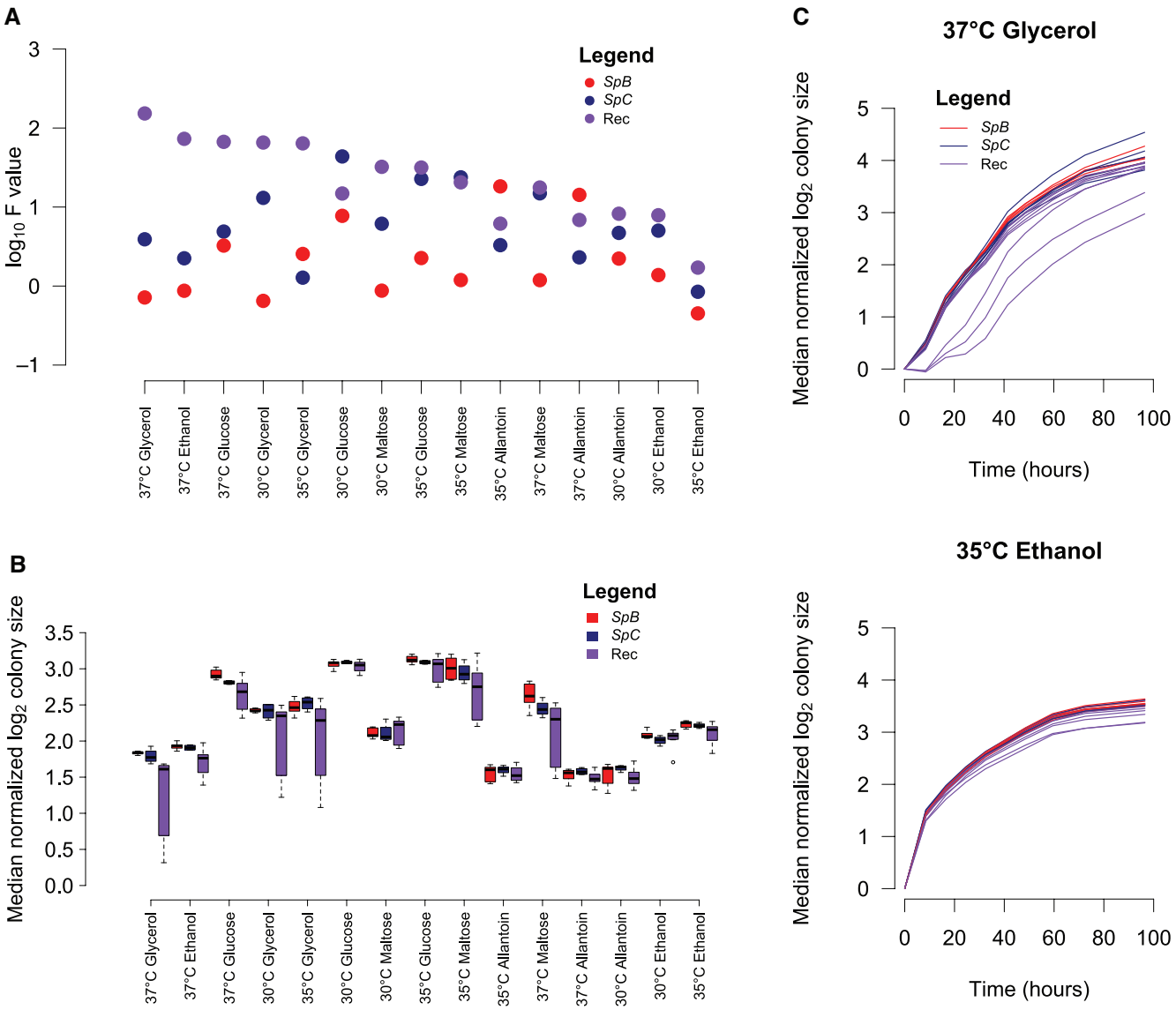

FIG. 4. Recombinant mtDNA in experimental diploid hybrids contribute to phenotypic variation. (*A*) Ranking of the environmental conditions according to the maximal *F* values, regardless of the mtDNA haplotype category. *F*-values were obtained from independent ANOVAs performed on each combination of mitochondrial haplotype category and environmental condition (red: *SpB*, blue: *SpC*, purple: recombinant mtDNA haplotypes). (*B*) Growth rate estimates for each combination of mtDNA haplotype category and environmental condition. The median value of the technical replicates for each strain within mtDNA haplotype categories was used. (*C*) Examples of growth curves of the individual strains for the conditions that have the highest (top) and lowest (bottom) maximal *F* values, respectively 37 °C glycerol and 35 °C ethanol.

interactions between a mitochondrial allele from one species and the nuclear allele of the other. Finally, incompatibilities could also arise from higher-order epistatic interactions between combinations of mitochondrial and nuclear alleles of the two parental genotypes.

Conclusion

The distribution of polymorphisms and mobile elements in mitochondrial genomes indicate that extensive exchanges took place between American *S. paradoxus* lineages during the recent speciation event by hybridization (Leducq et al. 2016). Such complex patterns are undoubtedly shaped by the high frequency of mtDNA recombination in yeast, which is a consequence of its biparental mtDNA transmission mode and transient heteroplasmy. A recent study on the frequency and distribution of mtDNA recombination hotspots in *S. cerevisiae* showed that the rate of recombination in this species is much higher than the rate of mutation (Fritsch et al. 2014). Fungal mitochondrial genomes are highly variable in size, content and architecture both within species and across long evolutionary distances (Aguileta et al. 2014; Freel et al. 2015) and the high rate of recombination could contribute to this rapid evolution (Fritsch et al. 2014). However, recombination will have effects on phenotypic diversity if enough divergence has accumulated in the parental mitochondrial genomes prior to recombination and if the hybridizing lineages give rise to viable progeny. Our results show that recombinant mitochondria were produced after hybridization between lineages that have diverged for more than a hundred

thousand years and are still segregating in a successful hybrid lineage. Future investigations should determine the generality of mitochondrial recombination during other hybridization events among natural yeast populations that have recently been revealed (Barbosa et al. 2016; Peris et al. 2016)

The numerous mitochondria-related functions that rely on both nuclear and mitochondrial genes (oxidative phosphorylation, mtDNA replication, mitochondrial transcription, and translation) suggest that co-evolution between the two genomes may be an important player in the emergence of genetic incompatibilities between diverged populations (Burton and Barreto 2012). Studies on inter and intraspecific hybrids between *Saccharomyces* yeasts revealed many BDMIs between mitochondrial and nuclear genes that reduce the fitness of hybrids (Lee et al. 2008; Chou et al. 2010; Albertin et al. 2013; Hou et al. 2015; Jhuang et al. 2017). Here, we did not attempt to determine whether the mitochondria themselves may have contributed to the reproductive isolation of the parental lineages *SpB* and *SpC* or between the hybrid lineage and these parents. However, we did show that mitochondrial recombination is likely to result in phenotypic changes. In our experiments, most of these changes resulted in reduced growth rates, suggesting that most mitochondrial recombinants could be deleterious to fitness in nature, although in a condition-dependent manner. Like point mutations, which under nearly-neutral theory tend to be slightly deleterious, most recombination events could be deleterious, while a small minority could be adaptive. The fact that the *SpC** hybrid lineage has persisted for several thousands of years with a recombinant nuclear and mitochondrial genome suggests that some might confer adaptation to unmeasured niches in the wild.

Mitochondrial recombination could also play a role in alleviating BDMIs between parental lineages *SpC* and *SpB* while allowing for adaptive introgression. BDMIs between mitochondrial and nuclear genomes have been shown to play an important role in reproductive isolation between yeast species (Lee et al. 2008; Chou et al. 2010; Albertin et al. 2013; Hou et al. 2015; Jhuang et al. 2017). A phase of heteroplasmy, recombination and mitotic selection of recombinant mtDNA upon return to growth after mating could eliminate BDMIs. For example, the *SpC** hybrids could have carried *SpB*-derived mitochondrial genome containing adaptive alleles and other alleles incompatible with *SpC* nuclear genes. Recombination between the *SpC* and *SpB* mtDNAs in the hybrids could have led to the maintenance of the adaptive *SpB* alleles while purging those involved in mt-*SpB* nuclear-*SpC* incompatibilities. Recombination of mtDNA among incipient yeast species can therefore contribute to complex evolutionary dynamics.

Several non-adaptive mechanisms could also contribute to the complex pattern of mitochondrial genome evolution observed in *SpC**. For instance, Ma and O'Farrell (2016) showed that mtDNA recombination in *Drosophila* could lead to the introgression of genomic regions responsible for the selfish propagation of certain mtDNAs, yielding recombinant mtDNAs in turn capable of selfish drive. In *S. cerevisiae*, several cellular mechanisms were shown to regulate mtDNA transmission in heteroplasmic stages, for instance by preventing the transmission of mitochondria with lower redox potential, responsible for cell aging (McFaline-Figueroa et al. 2011) or by limiting the propagation advantage of selfish mtDNA mutants (Karavaeva et al. 2017), suggesting a complex interplay between levels of mitochondrial activity and replication advantages. In the *SpB* × *SpC* diploid, some recombinant mtDNAs may have acquired a replicative advantage that led to their overrepresentation in the early heteroplasmic lineage, increasing their probability of becoming fixed as the lineages became homoplasmic. Such selfish behavior could explain the frequent reduced growth rates associated with recombinant mtDNAs, which could have been transmitted despite their net disadvantages on growth performance. Finally, the pattern of polymorphism in mitochondrial mobile elements like introns follows the pattern on mtDNA recombination in hybrids, suggesting that, as it was observed for mtDNA gene transfer among fungi and plants (Beaudet et al. 2013), these mobile elements could contribute to mtDNA evolution during hybridization in yeasts.

Materials and Methods

Mitochondrial Genome Assembly

We reconstructed mitochondrial genomes for a representative subsample of 22 *S. paradoxus* strains from North-east America (Supplementary material 1). On the basis of nuclear genome analysis (Leducq et al. 2016), strains were assigned to the European lineage *SpA* recently introduced in North America ($n = 3$), to the native American lineages *SpB* ($n = 10$) and *SpC* ($n = 6$) and to the American hybrid lineage *SpC** ($n = 3$). We retrieved mitochondrial scaffolds previously assembled and identified in these strains (Leducq et al. 2016). Briefly, reads from high coverage genome sequencing (~100×; Truseq Illumina; BioProject number PRJNA277692, BioSamples SAMN03389655–SAMN03389678) were assembled using ABySS (Simpson et al. 2009) with $k = 64$ (k-mer length). Mitochondrial fragments were identified by aligning and reordering all assembled scaffolds longer than 200 bp onto the *S. paradoxus* strain CBS432 reference mitochondrial genome (lineage *SpA*; GenBank accession: JQ862335.1; Prochazka et al. 2012) for each strain separately, using the "Move contigs" option implemented in MAUVE (Darling et al. 2004) with default parameters (minimum LCB weight = 200 bp). Because many of these strains had multiple mitochondrial scaffolds (only 12 mtDNA consisted of a single scaffold that could be manually circularized; see supplementary table S2, Supplementary Material online), we performed new genome assemblies using the IDBA_ud software (Peng et al. 2012). We used the default options for IDBA-ud's parameter settings: a minimum k-mer size of 20 and maximum k-mer size of 100, with 20 increments in each iteration. Our newly assembled mitochondrial scaffolds were identified as described above. Using IDBA_ud, 20 mtDNA consisted in a single scaffold that could be manually circularized, and two mitochondria only consisted in two overlapping scaffolds (see supplementary table S2, Supplementary Material online). We further used these assemblies for the following analyses. We

manually reconstructed mtDNAs in MEGA5 (Tamura et al. 2011), using CBS432 (*SpA*), UTM6 (*SpB*), and LL2011_003 (*SpC*) as references to merge contiguous scaffolds. Uncertain fusions were completed by sequences of "*n*". Genome assemblies were deposited on NCBI under accession numbers KY287641–KY287662 (see supplementary table S2, Supplementary Material online).

Read Mapping and Variant Calling

We aligned published whole-genome sequencing paired-end reads from 127 North-American *S. paradoxus* strains [23] on our de novo assembly of mtDNA from the *SpB* strain LL2012_022 using the Bowtie2 (Langmead and Salzberg 2012) software with default parameters. We chose this strain as a reference because among *SpB*, *SpC*, and *SpC** strains, its assembly is the largest and presents the most complete catalog of mobile elements (see supplementary fig. S4A, Supplementary Material online). We marked duplicated reads in the alignments with Picard (http://broadinstitute.github.io/picard/) and called variant sites in all strains at once using FreeBayes (https://arxiv.org/abs/1207.3907) with a ploidy parameter of 1. We filtered the resulting sites and genotypes with VCFtools (Danecek et al. 2011), keeping only sites with a quality score (QUAL field) above 20 and genotypes with a sequencing depth (DP field) above 3. We removed sites that were variable for the mapping of reads from strain LL2012_022 on LL2012_022 mtDNA assembly, as those could result from mapping errors or heterozygote sites. We also removed sites showing incongruent genotypes between duplicated libraries from five strains from different lineages to control for additional sequencing and mapping errors (Supplementary material 1). To visualize incomplete lineage sorting during the evolutionary history of mitochondrial CDS, we used SplitsTree with default parameters (Huson and Bryant 2006). We performed a STRUCTURE analysis (Falush et al. 2003) using variable positions to detect the most likely number of populations (*K*) tested in the range 1–10. Analyses were carried out under the admixture model over 10,000 iterations of the MCMC chain with a 20,000 burn-in period (10 independent runs per *K* value). We detected the most likely *K* value based on the Delta *K* method (Evanno et al. 2005).

Synteny among Complete Mitochondria

To identify potential mitochondrial rearrangements within and among *S. paradoxus* lineages, we determined the synteny between mitochondria of representative strains from each *S. paradoxus* lineages (Asian lineage: $n = 1$; *SpA*: $n = 2$; *SpB*: $n = 2$; *SpC*: $n = 2$; *SpC**: $n = 2$), using *S. cerevisiae* ($n = 2$) and *S. eubayanus* ($n = 1$) as outgroups. For each mitochondrion, we reported all possible 20 bp sequences in both strands and their coordinates. To avoid multiple matches due to repeated motifs and short duplications, and to shorten the computation time, we removed redundant sequences, that is, sequences having 100% match within and between strands, resulting in the removing of 5.1–11.8% sequences per mitochondrion. Then, for each pair of strains, we identified sequences having one-to-one 100% match and reported their coordinates in both mitochondria. All analyses were performed in R (R-Development-Core-Team 2011).

Mitochondrion Annotation

We performed de novo annotation for our 22 assembled mitochondria plus 16 complete mitochondria from the literature from a representative subset of outgroups (*S. cerevisiae*: $n = 4$; *S. eubayanus*: $n = 6$) and *S. paradoxus* lineages (Asian lineage: $n = 2$; *SpA*: $n = 3$; *SpB*: $n = 1$; see supplementary table S1, Supplementary Material online). Annotations for the 16 aforementioned mtDNA were already available but not homogeneous due to the different published methods. Each mitochondrion was annotated independently using MFannot tool set for Yeast Mitochondrial (http://megasun.bch.umontreal.ca/cgi-bin/mfannot/mfannotInterface.pl).

CDS that were detected but not annotated by MFannot were systematically searched by blast in the NCBI database for identification and manual annotation. These CDS mostly consisted in maturase-like genes located 3′ of genes *atp6* (*rf3*), *cox2* (*rf2*), and *cox3* (*cox3:3p*), or within introns of genes *cox1* and *cob*. To identify more accurately these CDS and the bounder of introns, we performed local alignments of these regions using conserved CDS as anchors (*atp6*, *cox2* and cox3; *cox1* and *cob* exons). We validated the absence of CDS and intron in a strain when a gap was found at its putative position. Otherwise, we determined whether the miss-annotation resulted from diverging sequence (e.g., premature stop codon, partial deletion) or imperfect assembly. We manually modified the annotation accordingly.

Evolution of Mitochondria Based on Concatenated CDS

We inferred the evolutionary history of the 38 annotated *Saccharomyces* mitochondria based upon the concatenated nucleotide alignment of conserved mitochondrial CDS (*atp6*, *atp8*, *atp9*, *cox2*, *cox3*, *rps3*) and exons (*cox1* and *cob*), for a total length of 6,357 bp. We established the global phylogeny using a Neighbor-Joining method (bootstrap test, $n = 1{,}000$ permutations). Evolutionary distances were based on a maximum composite likelihood model. Analyses were performed in MEGA6 (Tamura et al. 2013). We performed a STRUCTURE analysis (Falush et al. 2003) using variable positions observed in the alignment of the 38 concatenated sequences (602 variable positions) to detect the most likely number of populations (*K*) tested in the range 1–10. Analyses were carried out under the admixture model over 10,000 iterations of the MCMC chain with a 20,000 burn-in period (10 independent runs per *K* value). We detected the most likely *K* value based on the Delta *K* method (Evanno et al. 2005).

Identification of Introgression Based on North American Complete Mitochondria Alignment

The 20 complete and annotated mitochondria from North American lineage (including YPS138; Wu and Hao 2015; *SpB*: $n = 11$; *SpC*: $n = 6$; *SpC**: $n = 3$) were manually aligned together in MEGA5 (Tamura et al. 2011), using CDS as anchors. Highly diverging regions were aligned separately from the full

alignment using flanking conserved regions (CDS) as anchors, with default ClustalW parameters with following modifications for both Pairwise and Multiple Alignments: Gap Opening Penalty = 2; Gap Extension Penalty = 6.66, and Transition Weight = 0 to take into account the low GC content in the mitochondrion. The alignment was then curated manually. We performed a STRUCTURE analysis (Wu and Hao 2015) using variable positions observed in the alignment of the 20 aligned mitochondria (2,052 variable positions) to detect the most likely number of populations (K) tested in the range 1–7. Analyses were carried out as described above. On the basis of the above alignment, we identified potential introgressions from one parental lineage *SpB* or *SpC* in the hybrid lineage *SpC** (Leducq et al. 2016). First, we divided the alignment in discrete 750 bp windows, within which we identified sites that are overall polymorphic but either fixed in *SpB* strains (B-sites) or fixed in *SpC* strains (C-sites). We removed from these categories strains that showed admixture for the most likely K number of populations in the STRUCTURE analysis. From *SpC*, we excluded the strain YPS667 that is highly divergent from other *SpC* strain at the nuclear genome level (Leducq et al. 2016). We counted the total number of variable sites in each category and for each window (nB and nC, respectively). Then, for each strain i an each window, we calculated the number of B-sites (n_iB) and C-sites (n_iC) that are variable and defined the window as "B-like" (i.e., likely inherited by *SpB*) when $n_iB/nB > n_iC/nC$ (blue), or as "C-like" in the opposite case (i.e., likely inherited by *SpC*; red). We could not infer ancestry for following cases: $n_iB/nB = n_iC/nC$ (purple); $nB = 0$ or $nC = 0$ (black).

Generation of Hybrid Strains

SpB × *SpC* hybrid strains (see supplementary table S3, Supplementary Material online) were generated by allowing haploid strains (initial OD_{595}: 0.025 ml^{-1} each) to mate in YPD (1% yeast extract, 2% tryptone, 2% glucose) at 30 °C in shaking incubator for 4 h. Selection for diploid cells and loss of heteroplasmy was performed by three 24 h passages in $YPD_{G418\ Nat}$ (200 µg ml^{-1} geneticin, 100 µg ml^{-1} nourseothricin) at 30 °C in shaking incubator, diluting to OD_{595} ~0.005 ml^{-1} at each passage (~25–30 generations). Diploid cultures were plated on $YPD_{G418\ Nat}$ 2% agar and incubated at 30 °C. A single colony for each independent hybrid lineage was sampled to generate glycerol stocks.

mtDNA Extraction and Restriction Profiles

The method employed for mtDNA extraction is adapted from Defontaine et al. (1991). Strains were inoculated in 50 ml of YPGd (1% yeast extract, 2% tryptone, 3% glycerol, 0.2% glucose) and incubated at 30 °C in shaking incubator until $OD_{595} \sim 1.0\ ml^{-1}$. Cells were washed twice in sterile distilled water and once in 1.2 M sorbitol, 50 mM EDTA, and 2% 2-mercaptoethanol. Cells were resuspended in 5 ml of solution A (0.5 M sorbitol, 10 mM EDTA, 50 mM Tris, pH 7.5) with 2% 2-mercaptoethanol and 0.1 mg ml^{-1} zymolyase 20T and incubated at 37 °C for 3–4 h in shaking incubator for cell wall digestion. Cell debris were pelleted by centrifugation at 916 g for 13 min and mitochondria were pelleted from the supernatant by centrifugation at 15,000 × g for 15 min. Mitochondria pellets were washed four times with solution A to minimize genomic DNA contamination and lysed by resuspension in 100 mM NaCl, 10 mM EDTA, 50 mM Tris, and 1% N-lauroylsarcosine and incubation at room temperature for 1 h. Extraction of mtDNA was performed by phenol-chloroform extraction followed by ethanol precipitation. mtDNA samples were digested using *EcoRV* and *NdeI* restriction endonucleases (NEB) following the manufacturer's indications. Digested mtDNA fragments were separated by electrophoresis on 0.8% or 1% agarose gels at 4 V cm^{-1} for 2.5 or 3 h in TAE buffer with recirculation. Gels were stained with ethidium bromide.

PCR Assays for Validation of Parental mtDNA Haplotypes

We designed two pairs of PCR primers targeting mitochondrial coding loci that are polymorphic between the *SpB* and *SpC* strains used to generate the experimental hybrids (see supplementary table S3, Supplementary Material online). A 285 bp segment of the gene *atp6* was amplified using forward primer GGTTCAAGATGATTAATTTCACAAG and reverse primer ACCAGCAGGTACGAATAATGA with cycles as follows: 3 min at 94 °C; 40 times the following cycle: 30 s at 94 °C, 30 s at 57 °C, 25 s at 72 °C; 10 min at 72 °C. The *SpB* amplicon contains a restriction site for the enzyme *DpnII* generating 182 and 103 bp fragments, whereas the *SpC* amplicon contains no *DpnII* restriction site. Amplicon digestion was performed with *DpnII* (NEB) following the manufacturer's indications and the non-digested and digested amplicons were separated by agarose gel electrophoresis. A segment of the gene *rn1* was amplified using forward primer TGAGGTCCCGCATGAATGAC and the reverse primer ACGTACTTGTTTCACTCGTTTGT. The PCR reaction cycle was 3 min at 94 °C, 40 times the following cycle: 30 s at 94 °C, 30 s at 58 °C, and 50 s at 72 °C, and 10 min at 72 °C. The amplicons (716 bp for *SpB* and 762 bp for *SpC*) were separated by agarose gel electrophoresis.

Growth Measurement of the Hybrid Strains

SpB × *SpC* hybrid strains were printed in randomized 1,536 colonies arrays (24 technical replicates for each strain) on Omnitray plates containing media using a BM5-BC-48 colony processing robot (S&P Robotics Inc., Canada). The arrays were printed in triplicate on the following media: SCA (0.174% YNB, 2% glucose, 0.5% allantoin, 2% agar), SCM (0.174% YNB, 2% glucose, 0.5% maltose, 2% agar), YPD, YPE (1% yeast extract, 2% tryptone, 3% ethanol, 2% agar), and YPG (1% yeast extract, 2% tryptone, 3% glycerol, 2% agar). Plates were incubated 2 days at 30 °C, 35 °C or 37 °C. The colonies were replicated on the same media and incubated at the same temperature a second time. Pictures of the plates were taken immediately after the replication and after 8.5, 16.5, 24.5, 32.5, 41.5, 48.5, 59.5, 72.5 and 96.5 h of incubation. Colony size data were extracted from plates images using ImageJ 1.440 software (NIH) as described in Diss et al. (2013). For all technical replicates and conditions, the colony size values at each time

point were expressed in $\log_2$ and normalized by the colony size at time 0 expressed in $\log_2$.

Statistical Analysis of Growth Rate Estimates

One-factor ANOVAs were performed on normalized $\log_2$ colony sizes at 24.5 h, which correspond to growth rate estimates. Technical replicates for which there were no size values at 0 and/or 24.5 h (because of errors in the image analysis process) were filtered out for each condition individually. For each condition, the remaining number of replicates per strain was minimally 15/24, with an average of 22.5/24 across all conditions. Strains were grouped by mitochondrial haplotype (*SpB*, *SpC*, or recombinant). One-factor ANOVAs were performed separately on each combination of environmental condition and mtDNA haplotype category using the *anova.lm* function in R, with the identity of the strains as the factor tested (*SpB* = 5, *SpC* = 5, recombinant = 8). For further details about the ANOVA model used, see Supplementary material 4. To generate fig. 4*A*, the conditions were ranked according to the maximum F value obtained, regardless of the mtDNA haplotype category. The median of the technical replicates normalized $\log_2$ colony size values at 24.5 h for each strain in each condition was used to generate the boxplots in fig. 4*B*. The median of the technical replicates normalized $\log_2$ colony size values at each time point for each strain in 37 °C Glycerol and 35 °C Ethanol were used to generate the growth curves in fig. 4*C*.

Supplementary Material

Supplementary data are available at *Molecular Biology and Evolution* online.

Author Contributions

J.B.L. and C.R.L. designed research. J.B.L, L.N-T and Y.T analyzed data. M.H. performed experiments and analyzed results under the guidance of G.C. and C.R.L. J.B.P. and H.F. contributed reagents, methods and advice on the analysis and interpretation. J.B.L., C.R.L. and M.H. wrote the manuscript with input from all authors.

Acknowledgments

This work was supported by NSERC discovery and HFSP team grants to CRL. CRL holds the Canada Research Chair in Evolutionary Cell and Systems Biology. The authors thank Claude Lemieux for discussion, Louis-André Lortie for technical advice and two anonymous reviewers for their comments on the manuscript.

References

Aguileta G, de Vienne DM, Ross ON, Hood ME, Giraud T, Petit E, Gabaldon T. 2014. High variability of mitochondrial gene order among fungi. *Genome Biol Evol* 6:451–465.

Albertin W, da Silva T, Rigoulet M, Salin B, Masneuf-Pomarede I, de Vienne D, Sicard D, Bely M, Marullo P. 2013. The mitochondrial genome impacts respiration but not fermentation in interspecific *Saccharomyces* hybrids. *PLoS ONE* 8:e75121.

Baker E, Wang B, Bellora N, Peris D, Hulfachor AB, Koshalek JA, Adams M, Libkind D, Hittinger CT. 2015. The genome sequence of *Saccharomyces eubayanus* and the domestication of lager-brewing yeasts. *Mol Biol Evol* 32:2818–2831.

Barbosa R, Almeida P, Safar SV, Santos RO, Morais PB, Nielly-Thibault L, Leducq JB, Landry CR, Goncalves P, Rosa CA, et al. 2016. Evidence of natural hybridization in Brazilian wild lineages of *Saccharomyces cerevisiae*. *Genome Biol Evol* 8:317–329.

Barr CM, Neiman M, Taylor DR. 2005. Inheritance and recombination of mitochondrial genomes in plants, fungi and animals. *New Phytol* 168:39–50.

Barreto FS, Pereira RJ, Burton RS. 2015. Hybrid dysfunction and physiological compensation in gene expression. *Mol Biol Evol*. 32(3): 613–622.

Beaudet D, Terrat Y, Halary S, de la Providencia IE, Hijri M. 2013. Mitochondrial genome rearrangements in Glomus species triggered by homologous recombination between distinct mtDNA haplotypes. *Genome Biol Evol* 5:1628–1643.

Birky CW Jr. 2001. The inheritance of genes in mitochondria and chloroplasts: laws, mechanisms, and models. *Annu Rev Genet* 35:125–148.

Birky CW, Strausberg RL, Foster JL, Forster JL, Perlman PS. 1978. Vegetative segregation of mitochondria in yeast: estimating parameters using a random model. Molecular and *Gener Genet* 158:251.

Breton S, Stewart DT. 2015. Atypical mitochondrial inheritance patterns in eukaryotes. *Genome* 58:423–431.

Burton RS, Barreto FS. 2012. A disproportionate role for mtDNA in Dobzhansky–Muller incompatibilities? *Mol Ecol* 21:4942–4957.

Burton RS, Pereira RJ, Barreto FS. 2013. Cytonuclear genomic interactions and hybrid breakdown. *Ann Rev Ecol Evol Syst* 44:281–302.

Charron G, Leducq JB, Landry CR. 2014. Chromosomal variation segregates within incipient species and correlates with reproductive isolation. *Mol Ecol* 23:4362–4372.

Chou JY, Hung YS, Lin KH, Lee HY, Leu JY. 2010. Multiple molecular mechanisms cause reproductive isolation between three yeast species. *PLoS Biol* 8:e1000432.

Danecek P, Auton A, Abecasis G, Albers CA, Banks E, DePristo MA, Handsaker RE, Lunter G, Marth GT, Sherry ST. 2011. The variant call format and VCFtools. *Bioinformatics* 27:2156–2158.

Darling AC, Mau B, Blattner FR, Perna NT. 2004. Mauve: multiple alignment of conserved genomic sequence with rearrangements. *Genome Res* 14:1394–1403.

Defontaine A, Lecocq FM, Hallet JN. 1991. A rapid miniprep method for the preparation of yeast mitochondrial DNA. *Nucleic Acids Res* 19:185.

Diss G, Dube AK, Boutin J, Gagnon-Arsenault I, Landry CR. 2013. A systematic approach for the genetic dissection of protein complexes in living cells. *Cell Rep* 3:2155–2167.

Evanno G, Regnaut S, Goudet J. 2005. Detecting the number of clusters of individuals using the software STRUCTURE: a simulation study. *Mol Ecol* 14:2611–2620.

Falush D, Stephens M, Pritchard JK. 2003. Inference of population structure using multilocus genotype data: linked loci and correlated allele frequencies. *Genetics* 164:1567–1587.

Foury F, Roganti T, Lecrenier N, Purnelle B. 1998. The complete sequence of the mitochondrial genome of *Saccharomyces cerevisiae*. *FEBS Lett* 440:325–331.

Freel KC, Friedrich A, Schacherer J. 2015. Mitochondrial genome evolution in yeasts: an all-encompassing view. *FEMS Yeast Res* 15:fov023.

Fritsch ES, Chabbert CD, Klaus B, Steinmetz LM. 2014. A genome-wide map of mitochondrial DNA recombination in yeast. *Genetics* 198:755–771.

Gyllensten U, Wharton D, Josefsson A, Wilson AC. 1991. Paternal inheritance of mitochondrial DNA in mice. *Nature* 352:255–257.

Hittinger CT. 2013. *Saccharomyces* diversity and evolution: a budding model genus. *Trends Genet: TIG* 29:309–317.

Hou J, Friedrich A, Gounot JS, Schacherer J. 2015. Comprehensive survey of condition-specific reproductive isolation reveals genetic incompatibility in yeast. *Nat Commun* 6:7214.

Huson DH, Bryant D. 2006. Application of phylogenetic networks in evolutionary studies. *Mol Biol Evol* 23:254–267.

Jaramillo-Correa JP, Bousquet J. 2005. Mitochondrial genome recombination in the zone of contact between two hybridizing conifers. *Genetics* 171:1951–1962.

Jhuang HY, Lee HY, Leu JY. 2017. Mitochondrial–nuclear co-evolution leads to hybrid incompatibility through pentatricopeptide repeat proteins. *EMBO Rep* 18:87–101.

Karavaeva IE, Golyshev SA, Smirnova EA, Sokolov SS, Severin FF, Knorre DA. 2017. Mitochondrial depolarization in yeast zygotes inhibits clonal expansion of selfish mtDNA. *J Cell Sci*. 130(7):1274–1284.

Kodama Y, Kielland-Brandt MC, Hansen J. 2006. Lager brewing yeast. In: Comparative genomics: Springer. p. 145–164.

Kondo R, Satta Y, Matsuura ET, Ishiwa H, Takahata N, Chigusa SI. 1990. Incomplete maternal transmission of mitochondrial DNA in Drosophila. *Genetics* 126:657–663.

Kvist L, Martens J, Nazarenko AA, Orell M. 2003. Paternal leakage of mitochondrial DNA in the great tit (Parus major). *Mol Biol Evol* 20:243–247.

Landry CR, Townsend JP, Hartl DL, Cavalieri D. 2006. Ecological and evolutionary genomics of *Saccharomyces cerevisiae*. *Mol Ecol* 15:575–591.

Langmead B, Salzberg SL. 2012. Fast gapped-read alignment with Bowtie 2. *Nat Methods* 9:357–359.

Latorre-Pellicer A, Moreno-Loshuertos R, Lechuga-Vieco AV, Sánchez-Cabo F, Torroja C, Acín-Pérez R, Calvo E, Aix E, González-Guerra A, Logan A. 2016. Mitochondrial and nuclear DNA matching shapes metabolism and healthy ageing. *Nature* 535:561–565.

Leducq J-B, Nielly-Thibault L, Charron G, Eberlein C, Verta J-P, Samani P, Sylvester K, Hittinger CT, Bell G, Landry CR. 2016. Speciation driven by hybridization and chromosomal plasticity in a wild yeast. *Nat Microbiol* 1:15003.

Leducq JB, Charron G, Samani P, Dube AK, Sylvester K, James B, Almeida P, Sampaio JP, Hittinger CT, Bell G, et al. 2014. Local climatic adaptation in a widespread microorganism. *Proc Biol Sci/R Soc* 281:20132472.

Lee HY, Chou JY, Cheong L, Chang NH, Yang SY, Leu JY. 2008. Incompatibility of nuclear and mitochondrial genomes causes hybrid sterility between two yeast species. *Cell* 135:1065–1073.

Ma H, O'Farrell PH. 2016. Selfish drive can trump function when animal mitochondrial genomes compete. *Nat Genet* 48:798–802.

McFaline-Figueroa JR, Vevea J, Swayne TC, Zhou C, Liu C, Leung G, Boldogh IR, Pon LA. 2011. Mitochondrial quality control during inheritance is associated with lifespan and mother–daughter age asymmetry in budding yeast. *Aging Cell* 10:885–895.

Mossman JA, Tross JG, Li N, Wu Z, Rand DM. 2016. Mitochondrial-nuclear interactions mediate sex-specific transcriptional profiles in Drosophila. *Genetics* 116:192328.

Nakao Y, Kanamori T, Itoh T, Kodama Y, Rainieri S, Nakamura N, Shimonaga T, Hattori M, Ashikari T. 2009. Genome sequence of the lager brewing yeast, an interspecies hybrid. *DNA Res* 16:115–129.

Okuno M, Kajitani R., Ryusui R., Morimoto H., Kodama Y., & Itoh T. 2016. Next-generation sequencing analysis of lager brewing yeast strains reveals the evolutionary history of interspecies hybridization. *DNA Res* 23 (1): 67–80.

Paliwal S, Fiumera AC, Fiumera HL. 2014. Mitochondrial-nuclear epistasis contributes to phenotypic variation and coadaptation in natural isolates of *Saccharomyces cerevisiae*. *Genetics* 198:1251–1265.

Peng Y, Leung HC, Yiu S-M, Chin FY. 2012. IDBA-UD: a de novo assembler for single-cell and metagenomic sequencing data with highly uneven depth. *Bioinformatics* 28:1420–1428.

Peris D, Arias A, Orlić S, Belloch C, Perez-Traves L, Querol A, Barrio E. 2017. Mitochondrial introgression suggests extensive ancestral hybridization events among *Saccharomyces* species. *Mol Phylo Evol*. 108:49–60.

Peris D, Langdon QK, Moriarty RV, Sylvester K, Bontrager M, Charron G, Leducq JB, Landry CR, Libkind D, Hittinger CT. 2016. Complex ancestries of lager-brewing hybrids were shaped by standing variation in the wild yeast *Saccharomyces eubayanus*. *PLoS Genet* 12:e1006155.

Piskur J, Smole S, Groth C, Petersen RF, Pedersen MB. 1998. Structure and genetic stability of mitochondrial genomes vary among yeasts of the genus *Saccharomyces*. *Int J Syst Bacteriol* 48 (Pt 3): 1015–1024.

Prochazka E, Franko F, Polakova S, Sulo P. 2012. A complete sequence of *Saccharomyces paradoxus* mitochondrial genome that restores the respiration in *S. cerevisiae*. *FEMS Yeast Res* 12:819–830.

Querol A, Bond U. 2009. The complex and dynamic genomes of industrial yeasts. *FEMS Microbiol Lett* 293:1–10.

R-Development-Core-Team. 2011. R: a language and environment for statistical computing. In: R Foundation for Statistical Computing. Vienna, Austria, 2013. http://www. R-project.org, ISBN 3-900051-07-0.

Rainieri S, Kodama Y, Nakao Y, Pulvirenti A, Giudici P. 2008. The inheritance of mtDNA in lager brewing strains. *FEMS Yeast Res* 8:586–596.

Rokas A, Ladoukakis E, Zouros E. 2003. Animal mitochondrial DNA recombination revisited. *Trends Ecol Evol* 18:411–417.

Schumer M, Rosenthal GG, Andolfatto P. 2014. How common is homoploid hybrid speciation? *Evolution* 68:1553–1560.

Simpson JT, Wong K, Jackman SD, Schein JE, Jones SJ, Birol I. 2009. ABySS: a parallel assembler for short read sequence data. *Genome Res* 19:1117–1123.

Sniegowski PD, Dombrowski PG, Fingerman E. 2002. *Saccharomyces cerevisiae* and *Saccharomyces paradoxus* coexist in a natural woodland site in North America and display different levels of reproductive isolation from European conspecifics. *FEMS Yeast Res* 1:299–306.

Tamura K, Peterson D, Peterson N, Stecher G, Nei M, Kumar S. 2011. MEGA5: molecular evolutionary genetics analysis using maximum likelihood, evolutionary distance, and maximum parsimony methods. *Mol Biol Evol* 28:2731–2739.

Tamura K, Stecher G, Peterson D, Filipski A, Kumar S. 2013. MEGA6: molecular evolutionary genetics analysis version 6.0. *Mol Biol Evol* 30:2725–2729.

Wei W, McCusker JH, Hyman RW, Jones T, Ning Y, Cao Z, Gu Z, Bruno D, Miranda M, Nguyen M. 2007. Genome sequencing and comparative analysis of *Saccharomyces cerevisiae* strain YJM789. *Proc Natl Acad Sci U S A* 104:12825–12830.

Wilson AJ, Xu J. 2012. Mitochondrial inheritance: diverse patterns and mechanisms with an emphasis on fungi. *Mycology* 3:158–166.

Wolters JF, Chiu K, Fiumera HL. 2015. Population structure of mitochondrial genomes in *Saccharomyces cerevisiae*. *BMC Genomics* 16:451.

Wu B, Hao W. 2015. A dynamic mobile DNA family in the yeast mitochondrial genome. *G3: Genes| Genomes| Genetics* 5:1273–1282.

Xu J, Wang P. 2015. Mitochondrial inheritance in basidiomycete fungi. *Fungal Biol Rev* 29:209–219.

Xu J, Yan Z, Guo H. 2009. Divergence, hybridization, and recombination in the mitochondrial genome of the human pathogenic yeast *Cryptococcus gattii*. *Mol Ecol* 18:2628–2642.

Zhu CT, Ingelmo P, Rand DM. 2014. GxGxE for lifespan in Drosophila: mitochondrial, nuclear, and dietary interactions that modify longevity. *PLoS Genet* 10:e1004354.